

CS 957, System-2 AI Large Concept Models

Mohammad Hossein Rohban

June. 2025

Sharif University of Technology

Motivation

- Explicit reasoning and planning at **multiple levels of abstraction**
- Researchers do not usually prepare detailed speeches by **writing out every single word** they will pronounce
- If probability of correct token generation is p , for a sequence of length L , the probability of generating a correct sentence would be roughly p^L

Let's brainstorm!

How to go about this?

Large Concept Models:

Language Modeling in a Sentence Representation Space

The LCM team, Loïc Barrault^{*}, Paul-Ambroise Duquenne^{*}, Maha Elbayad^{*}, Artyom Kozhevnikov^{*}, Belen Alastruey[†], Pierre Andrews[†], Mariano Coria[†], Guillaume Couairon^{+†}, Marta R. Costa-jussà[†], David Dale[†], Hady Elsahar[†], Kevin Heffernan[†], João Maria Janeiro[†], Tuan Tran[†], Christophe Ropers[†], Eduardo Sánchez[†], Robin San Roman[†], Alexandre Mourachko[‡], Safiyyah Saleem[‡], Holger Schwenk[‡]

FAIR at Meta

^{*}Core contributors, alphabetical order, [†]Contributors to data preparation, LCM extensions and evaluation, alphabetical order, [‡]Research and project management, alphabetical order, ⁺Initial work while at FAIR at Meta, new affiliation: INRIA, France

Overview

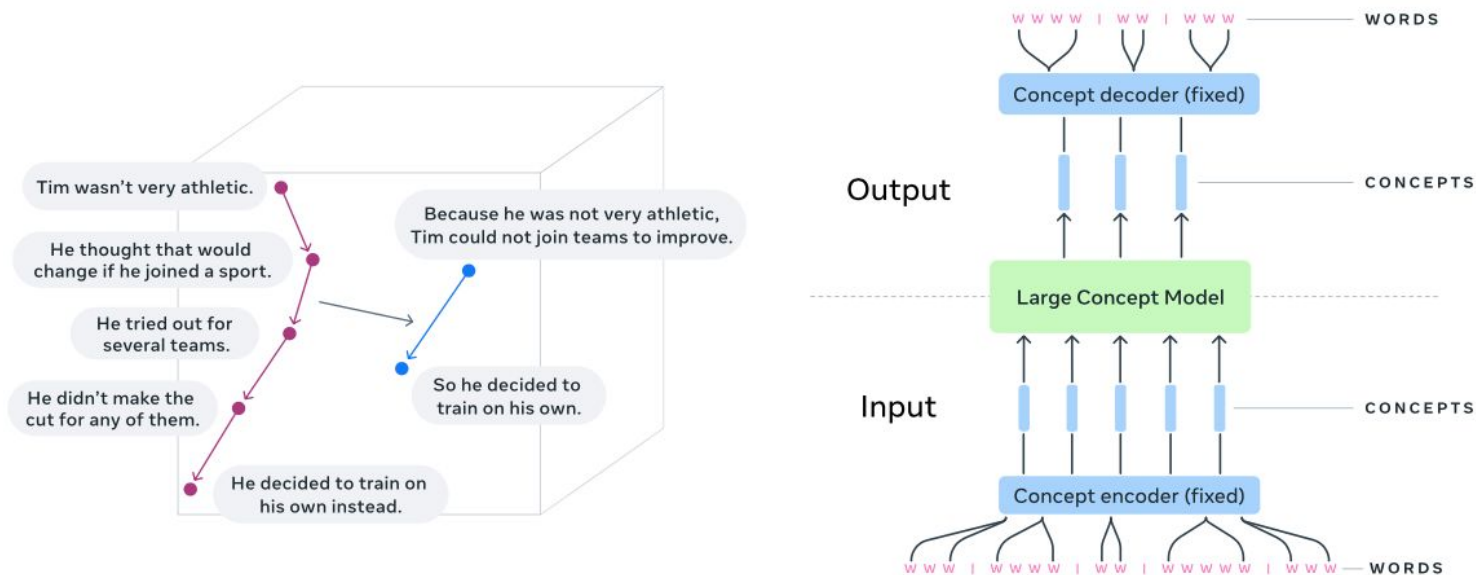


Figure 1 - Left: visualization of reasoning in an embedding space of concepts (task of summarization).
Right: fundamental architecture of an LARGE CONCEPT MODEL (LCM).

★: concept encoder and decoder are frozen.

Benefits

- Shorter sequence
 - Less computational overhead
- Language agnostic
- Modality Agnostic
 - Avoiding modality competition

Multi-lingual and Multi-Modal

| Model | Text | | Speech | | Image | | Video | |
|--------------|-------|--------|--------|--------|-------|--------|-------|--------|
| | Input | Output | Input | Output | Input | Output | Input | Output |
| GEMINI | 47 | 47 | 62 | ✓ | ✓ | ✓ | ✓ | ✗ |
| GPT | 85 | 85 | ✓ | ✓ | ✓ | ✓ | ? | ✗ |
| CLAUDE | 37 | 37 | ✓ | ✓ | ✓ | ✓ | ✗ | ✗ |
| BLOOM | 46 | 46 | ✗ | ✗ | ✓ | ✓ | ✗ | ✗ |
| LLAMA 3-400B | 8 | 8 | 34 | ✗ | ✓ | ✓ | ✗ | ✗ |
| LCM-SONAR | 200 | 200 | 76 | 1 | ✗ | ✗ | (ASL) | ✗ |

Table 1 - Comparison of language and modality coverage for several LLMs and our LCM operating on the SONAR embedding space. SONAR has an experimental support for American Sign Language (ASL) which is not used in this paper.

SONAR Encoding

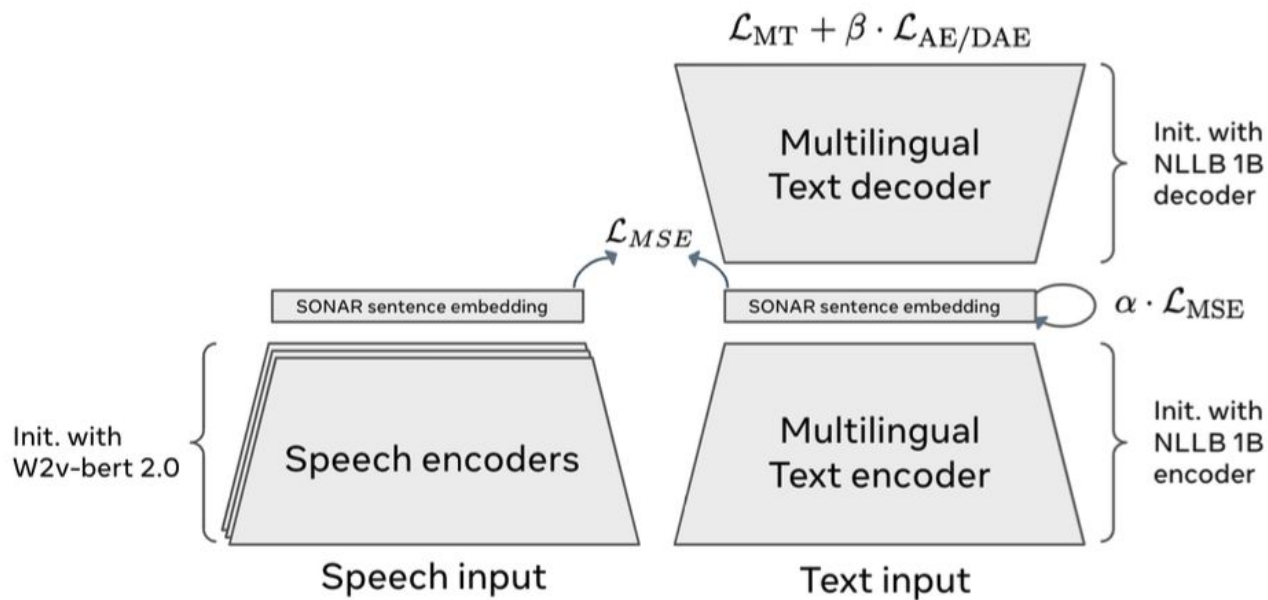


Figure 2 - Encoder/decoder bottleneck architecture to train the SONAR text embeddings (right part of figure). Teacher-student approach to extend SONAR to the speech modality (left part).

Sentence Segmentation

1. SpaCy segmenter (SPACY): Rule-based; relies on **punctuation** and **capitalization**; suitable for **high-resource languages**
2. Segment any Text (SAT): **predict** sentence boundaries at the token level; less reliant on **punctuation** and **capitalization**
3. Force a length cap on the sentences to make them short.

How to evaluate these segmentors?

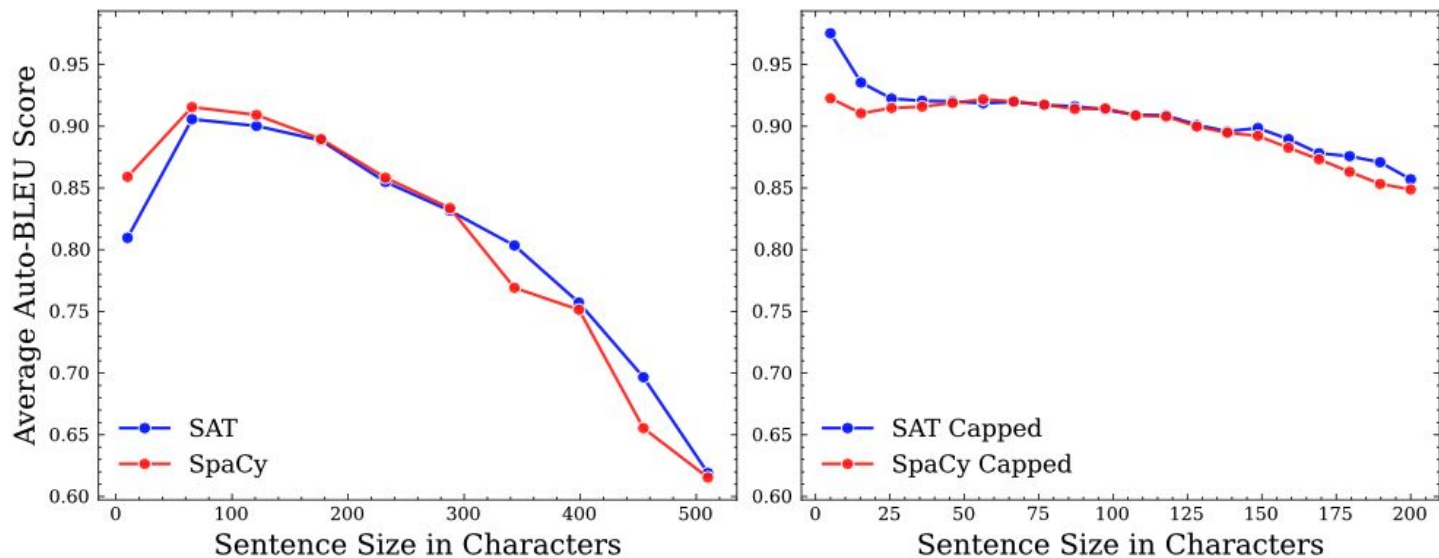


Figure 3 - Segmenters quality. Average Auto-BLEU scores for different sentence segmentation methods depending on sentence length, for both out of the box (left) and capped implementations (right).

Base LCM

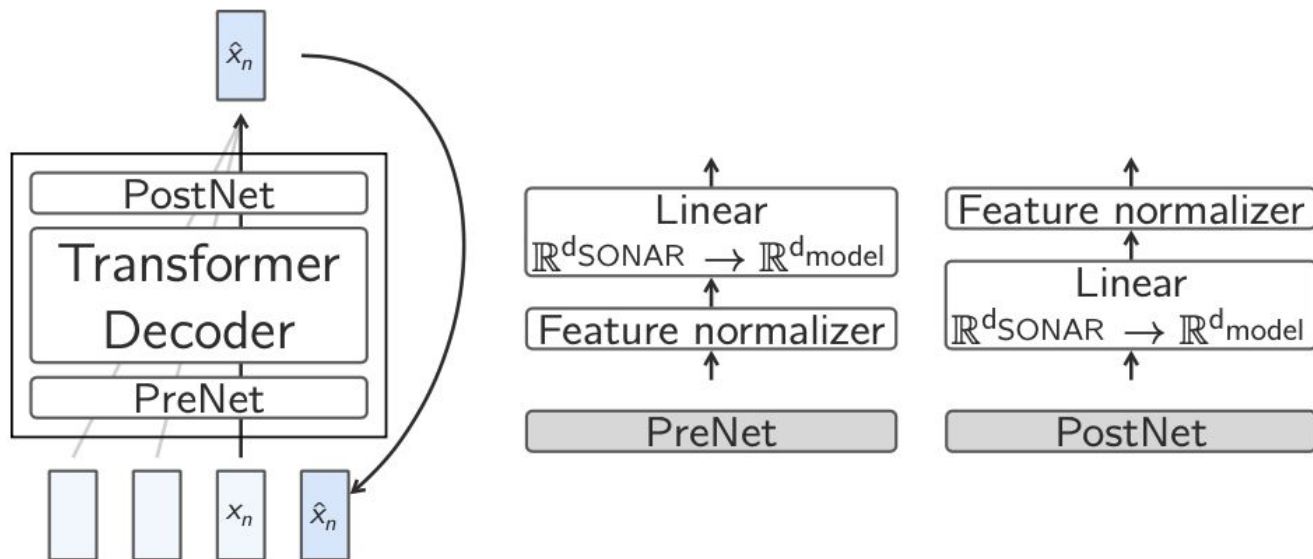


Figure 4 - TheBase-LCM. Illustration of the BASE-LCM. At its core is a standard decoder-only Transformer surrounded with a PreNet and a PostNet.

Details

$$\text{PreNet}(\mathbf{x}) = \text{normalize}(\mathbf{x}) \mathbf{W}_{\text{pre}}^t + \mathbf{b}_{\text{pre}},$$

$$\text{PostNet}(\mathbf{x}) = \text{denormalize}(\mathbf{x} \mathbf{W}_{\text{post}}^t + \mathbf{b}_{\text{post}}),$$

$$\text{normalize}(\mathbf{x}) = \frac{\mathbf{x} - \boldsymbol{\mu}}{\boldsymbol{\sigma}}, \quad \text{denormalize}(\mathbf{x}) = \boldsymbol{\mu} + \boldsymbol{\sigma} \mathbf{x}.$$

$$\hat{\mathbf{x}}_n = f(\mathbf{x}_{<n}; \boldsymbol{\theta}), \quad \text{MSE}(\hat{\mathbf{x}}_n, \mathbf{x}_n) = \|\hat{\mathbf{x}}_n - \mathbf{x}_n\|^2.$$

$$\mathcal{L}_{\text{BASE-LCM}}(\boldsymbol{\theta}) = \mathbb{E}_{\mathbf{x} \sim q} \left[\sum_{n=1}^{|\mathbf{x}|} \text{MSE}(f(\mathbf{x}_{<n}; \boldsymbol{\theta}), \mathbf{x}_n) \right].$$

What are the potential problems with base LCM?

Let's brainstorm

Diffusion-based LCM

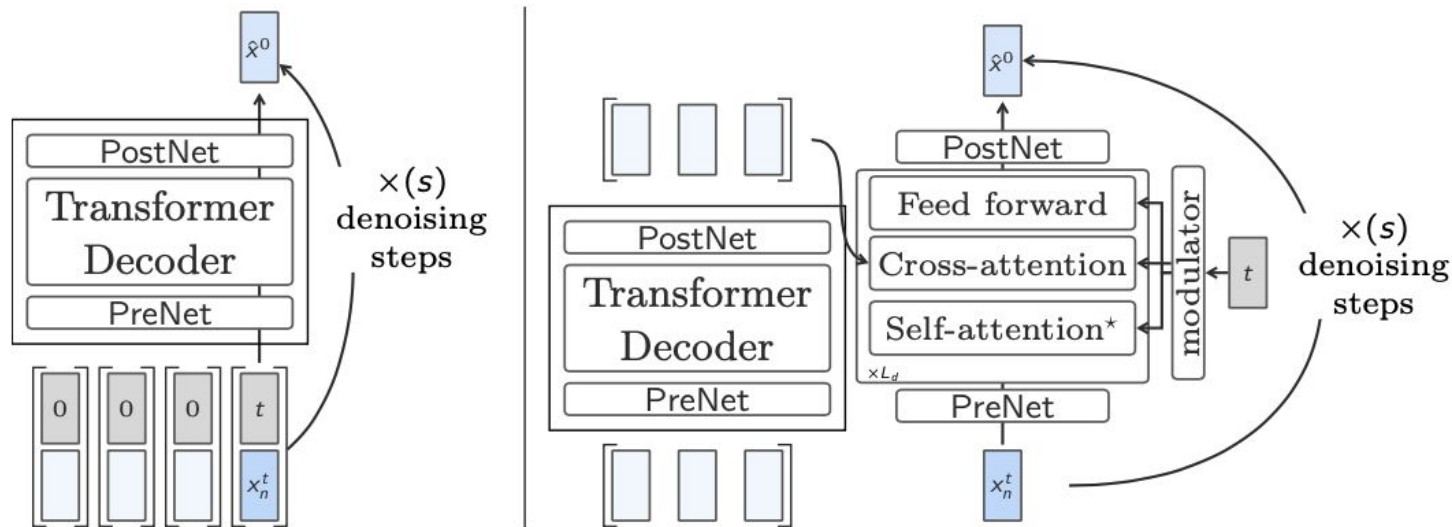


Figure 6 - Inference with diffusion-based LCMs. In the left-hand side, an illustration of the ONE-TOWER LCM and on the right-hand side an illustration of the TWO-TOWER LCM.

Details

$$q(\mathbf{x}^t|\mathbf{x}^0) := \mathcal{N}(\alpha_t \mathbf{x}^0, \sigma_t^2 \mathbf{I}).$$

$$\mathbf{x}^t = \alpha_t \mathbf{x}^0 + \sigma_t \boldsymbol{\epsilon} \quad \text{where } \boldsymbol{\epsilon} \sim \mathcal{N}(\mathbf{0}, \mathbf{I})$$

$$\alpha_t^2 = \text{sigmoid}(\lambda_t), \quad \sigma_t^2 = \text{sigmoid}(-\lambda_t) = 1 - \text{sigmoid}(\lambda_t), \quad \lambda_t = \log(\alpha_t^2 / \sigma_t^2),$$

$$q(\mathbf{x}^{1\dots T}|\mathbf{x}^0) := \prod_{t=1}^T q(\mathbf{x}^t|\mathbf{x}^{t-1}), \quad q(\mathbf{x}^t|\mathbf{x}^{t-1}) := \mathcal{N}(\mathbf{x}^t; \sqrt{1 - \beta_t} \mathbf{x}^{t-1}, \beta_t \mathbf{I}),$$

$$\alpha_t^2 = \prod_{s=1}^t (1 - \beta_s).$$

Details

Cosine. The schedule formulated in [Nichol and Dhariwal \(2021\)](#) as:

$$\alpha_t^2 = f(t)/f(0), \text{ where } f(t) = \cos^2 \left(\frac{t+s}{1+s} \cdot \frac{\pi}{2} \right), \text{ where } s = 0.008. \quad (12)$$

Quadratic. The schedule introduced in [Ho et al. \(2020\)](#) where the variances $(\beta_t)_t$ are set to constants increasing quadratically from β_0 to β_1 .

$$\beta_{t/T} = \left(\sqrt{\beta_0} + \frac{t}{T} \cdot \left(\sqrt{\beta_1} - \sqrt{\beta_0} \right) \right)^2. \quad (13)$$

Sigmoid. We introduce in this work, the *sigmoid* schedule as a means to study the impact of the SNR distribution on the training of our models. The schedule is parametrized by two hyper-parameters (γ, δ) and is defined as:

$$\alpha_t^2 = f(t)/f(0), \text{ where } f(t) = \text{sigmoid}(\delta - \gamma \logit(t)), \quad (14)$$

Details

$$p_{\boldsymbol{\theta}}(\mathbf{x}^{0:T}) := p(\mathbf{x}^T) \prod_{t=1}^T p_{\boldsymbol{\theta}}(\mathbf{x}^{t-1} | \mathbf{x}^t), \quad p_{\boldsymbol{\theta}}(\mathbf{x}^{t-1} | \mathbf{x}^t) := \mathcal{N}(\mathbf{x}^{t-1}; \boldsymbol{\mu}_{\boldsymbol{\theta}}(\mathbf{x}^t, t), \boldsymbol{\Sigma}_{\boldsymbol{\theta}}(\mathbf{x}^t, t)),$$

$$\mathcal{L}(\boldsymbol{\theta}) := \mathbb{E}_{t \sim \mathcal{U}(0,1)} [\omega(t) \mathcal{L}(t, \boldsymbol{\theta})], \quad \mathcal{L}(t, \boldsymbol{\theta}) := \mathbb{E}_{\mathbf{x}^0, \boldsymbol{\epsilon}} \left[\|\mathbf{x}^0 - \boldsymbol{\mu}_{\boldsymbol{\theta}}(\alpha_t \mathbf{x}^0 + \sigma_t \boldsymbol{\epsilon}, t)\|_2^2 \right].$$

$$\omega(t) = \max(\min(\exp(\lambda_t), \lambda_{\max}), \lambda_{\min}), \quad \lambda_t = \log(\alpha_t^2 / \sigma_t^2),$$

$$\nabla_x \log_{\gamma} p(x|y) = (1 - \gamma) \nabla_x \log p(x) + \gamma \nabla_x \log p(x|y),$$

$$\mathcal{L}_{\text{fragility}}(\boldsymbol{\theta}) := \mathbb{E}_{t \sim \mathcal{U}(0,1), \mathbf{x}^0, \boldsymbol{\epsilon}} \left[\omega(\mathbf{x}^0) \|\mathbf{x}^0 - \boldsymbol{\mu}_{\boldsymbol{\theta}}(\alpha_t \mathbf{x}^0 + \sigma_t \boldsymbol{\epsilon}, t)\|_2^2 \right],$$

$$\omega(\mathbf{x}^0) = \text{sigmoid}(a \text{ fragility}(\mathbf{x}^0) + b),$$

Fragility

$$\begin{aligned}\text{fragility}(w) &:= -\mathbb{E}_{\alpha \sim \mathcal{U}([0,1]), \epsilon \sim \mathcal{N}(\mathbf{0}, \mathbf{I})} [\text{score}(w, w_{\alpha, \epsilon})], \\ \mathbf{x}_{\alpha, \epsilon} &= \text{denormalize}(\sqrt{1 - \alpha} \text{ normalize}(\mathbf{x}) + \sqrt{\alpha} \epsilon), \\ w_{\alpha, \epsilon} &= \text{decode}(\mathbf{x}_{\alpha, \epsilon}),\end{aligned}$$

Training One-Tower LCM

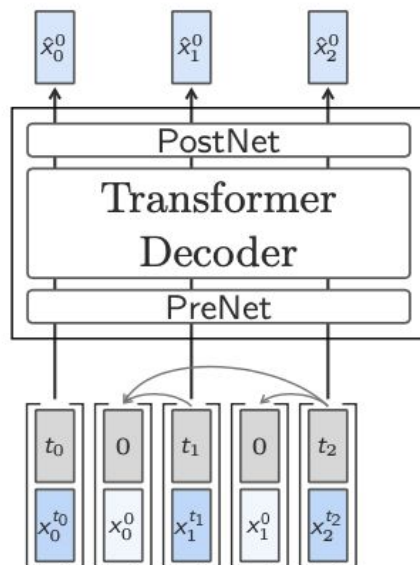


Figure 7 - Training of One-Tower diffusion LCM. Interleaving the clean and noisy embeddings and sampling different diffusion timesteps allows for efficient training.

Training Two-Tower LCM

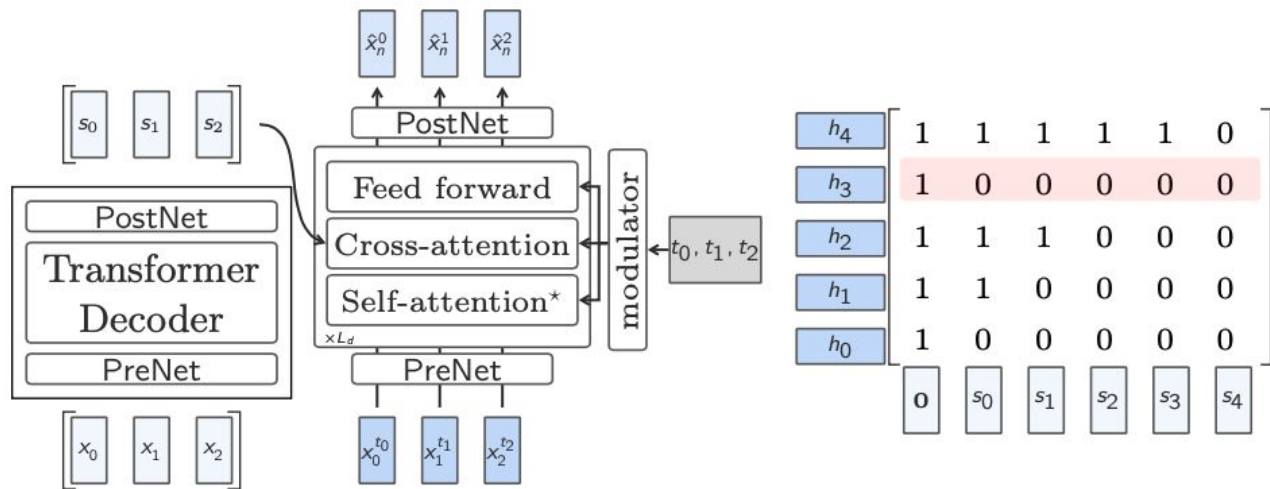


Figure 8 - Training Two-Tower diffusion LCM. On the left panel, a TWO-TOWER forward pass in training time in order to denoise multiple embeddings in parallel. On the right side panel a visualization of the denoiser’s cross-attention masks with the red highlighted row signaling a sample dropped to train the denoiser unconditionally. (h_1, \dots, h_4) denotes the sequence of intermediate representations in the denoiser right before the cross-attention layer.

Training Two-Tower LCM

dimension d_{model} . Each block of each Transformer layer in the denoiser (including the cross-attention layer) is modulated with adaptive layer norm (AdaLN, [Perez et al. \(2018\)](#); [Peebles and Xie \(2023\)](#)). The AdaLN modulator of TWO-TOWER regresses channel-wise scale (γ), shift (β) and residual gates (α) from the embedding of the current diffusion timestep t .

$$[\beta, \gamma, \alpha] = \text{SiLU}(\text{embed}(t))\mathbf{W}^t + \mathbf{b}, \quad (21)$$

$$\mathbf{y} = \mathbf{x} + \alpha \text{Block}((1 + \gamma)\mathbf{x} + \beta), \quad (22)$$

Efficiency of LCMs

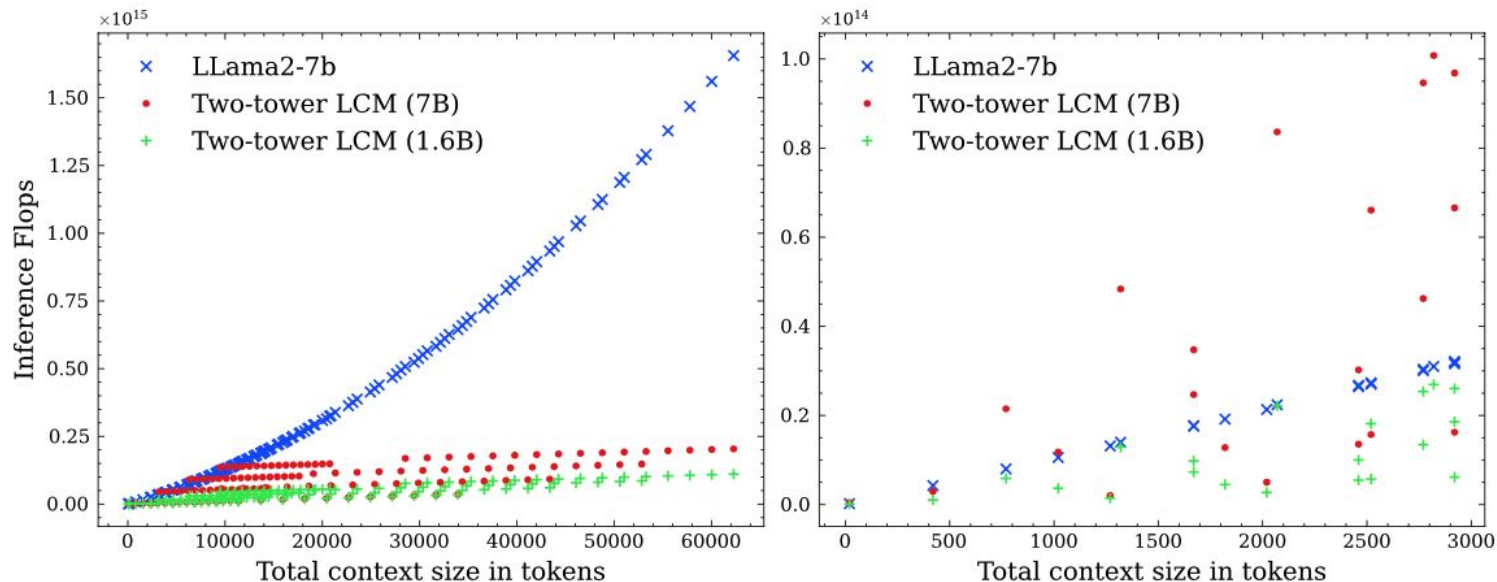


Figure 13 - Theoretical inference Flops of LCMs and LLMs. We evaluate the inference flops for different text lengths (in LLAMA2 tokens) with a variable average sentence length. Only extremely short sentences (≤ 10 tokens) favor LLMs.

Results

| MODEL | Paradigm | CNN DAILYMAIL | | | | | |
|--------------------|----------|---------------|--------------|--------------|--------------|--------------|--------------|
| | | R-L(↑) | OVL-3 (↑) | REP-4 (↓) | CoLA (↑) | SH-4 (↑) | SH-5 (↑) |
| Ground truth | — | 100.00 | 0.170 | 0.684 | 0.850 | 0.683 | 0.586 |
| T5-3B | SFT | 37.56 | 0.174 | 0.854 | 0.946 | 0.773 | 0.503 |
| GEMMA-7B-IT | IFT | 31.14 | 0.245 | 1.032 | 0.963 | 0.740 | 0.560 |
| MISTRAL-7B-v0.3-IT | IFT | 36.06 | 0.200 | 0.780 | 0.972 | 0.780 | 0.676 |
| LLAMA-3.1-8B-IT | IFT | 34.97 | 0.248 | 0.928 | 0.973 | 0.763 | 0.692 |
| TWO-TOWER-7B-IT | IFT | 36.47 | 0.177 | 0.757 | 0.767 | 0.723 | 0.459 |

| MODEL | Paradigm | XSUM | | | | | |
|--------------------|----------|--------------|--------------|--------------|--------------|--------------|--------------|
| | | R-L(↑) | OVL-3 (↑) | REP-4 (↓) | CoLA (↑) | SH-4 (↑) | SH-5 (↑) |
| Ground truth | — | 100.00 | 0.108 | 0.399 | 0.987 | 0.352 | 0.418 |
| T5-3B | — | 17.11 | 0.221 | 0.671 | 0.939 | 0.680 | 0.450 |
| GEMMA-7B-IT | IFT | 18.20 | 0.177 | 0.620 | 0.769 | 0.546 | 0.446 |
| MISTRAL-7B-v0.3-IT | IFT | 21.22 | 0.162 | 0.480 | 0.922 | 0.633 | 0.621 |
| LLAMA-3.1-8B-IT | IFT | 20.35 | 0.186 | 0.501 | 0.941 | 0.687 | 0.658 |
| TWO-TOWER-7B-IT | IFT | 23.71 | 0.106 | 0.464 | 0.683 | 0.358 | 0.284 |

Table 10 - Performance on the CNN DAILYMAIL and XSUM summarization tasks.

Results

| CNN DAILYMAIL | | | | | |
|--------------------|-----|--------------|--------------|--------------|--------------|
| METHOD | WR | R-L(↑) | OVL-3 (↑) | REP-4 (↓) | CoLA (↑) |
| GEMMA-7B-IT | 6.8 | 35.54 | 0.801 | 2.104 | 0.951 |
| MISTRAL-7B-v0.3-IT | 6.4 | 34.24 | 0.817 | 2.063 | 0.959 |
| LLAMA-3.1-8B-IT | 8.5 | 37.76 | 0.822 | 2.582 | 0.844 |
| TWO-TOWER-7B-IT | 6.3 | 30.85 | 0.726 | 2.911 | 0.474 |

| XSUM | | | | | |
|--------------------|------|--------------|--------------|--------------|--------------|
| METHOD | WR | R-L(↑) | OVL-3 (↑) | REP-4 (↓) | CoLA (↑) |
| GEMMA-7B-IT | 19.5 | 17.89 | 0.963 | 10.238 | 0.116 |
| MISTRAL-7B-v0.3-IT | 1.6 | 29.31 | 0.893 | 2.268 | 0.939 |
| LLAMA-3.1-8B-IT | 19.8 | 28.84 | 0.915 | 2.543 | 0.898 |
| TWO-TOWER-7B-IT | 7.1 | 23.82 | 0.561 | 1.542 | 0.603 |

Table 12 - Performance on the summary expansion tasks of CNN DAILYMAIL and XSUM, evaluated with the metrics described in Table 8. WR is the word count ratio between the hypothesis and the source summary.

Results

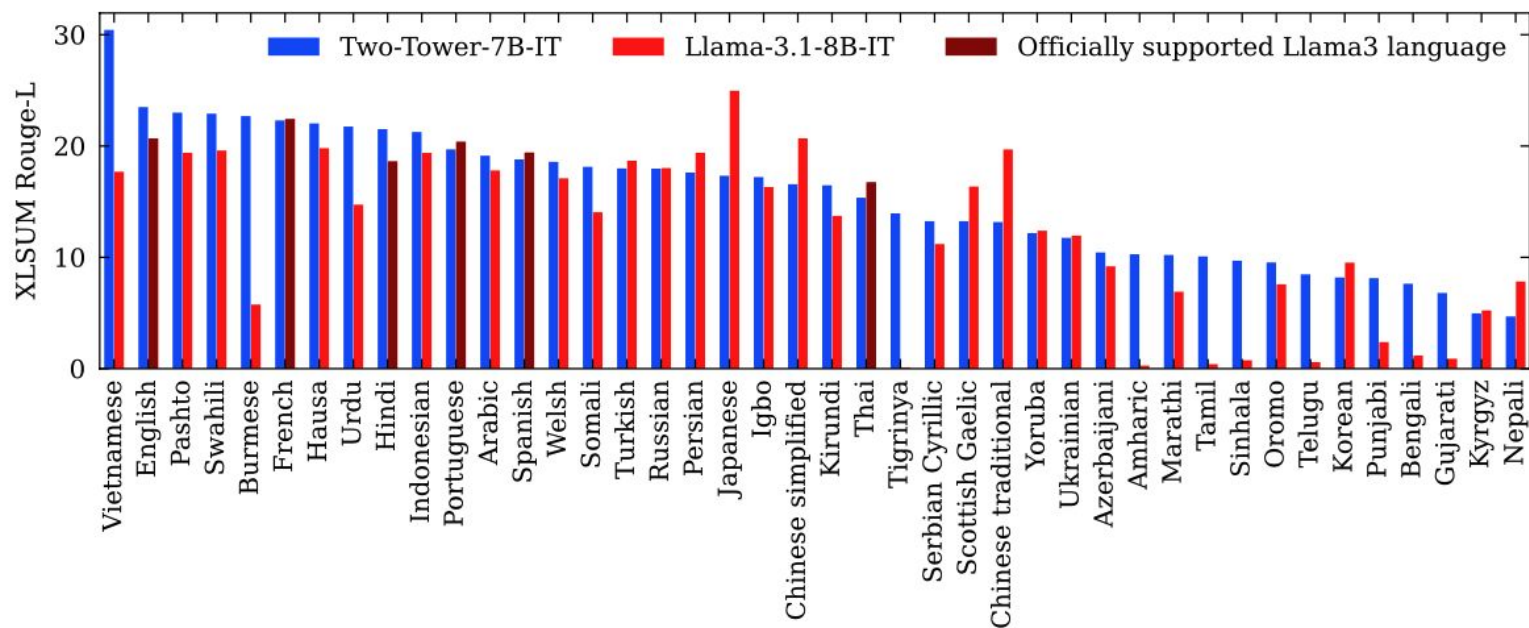


Figure 16 - ROUGE-L scores on XLSUM for LLAMA-3.1-8B-IT and TWO-TOWER-7B-IT.